Annals of Work Exposures and Health, 2018, Vol. 62, No. 6, 699–710
doi: 10.1093/annweh/wxy033
Advance Access publication 18 May 2018
Original Article

Original Article

Particle Concentrations in Occupational Settings Measured with a Nanoparticle Respiratory Deposition (NRD) Sampler

Larissa V. Stebounova[1], Natalia I. Gonzalez-Pech[2], Jae Hong Park[3], T. Renee Anthony[1], Vicki H. Grassian[2,4], and Thomas M. Peters[1]*

[1]Department of Occupational and Environmental Health, The University of 145 N Riverside Drive, Iowa, Iowa City, IA 52242, USA; [2]Department of Chemistry and Biochemistry, University of California San Diego, 9500 Gilman Dr., La Jolla, CA 92093, USA; [3]School of Health Sciences, Purdue University, 550 Stadium Mall Drive, West Lafayette, IN 47907, USA; [4]Department of Nanoengineering, Scripps Institution of Oceanography, University of California, 9500 Gilman Drive, La Jolla, CA 92093, USA

*Author to whom correspondence should be addressed. Tel: +1 319 335 4436; e-mail: thomas-m-peters@uiowa.edu

Submitted 19 December 2017; revised 16 March 2018; editorial decision 14 April 2018; revised version accepted 30 April 2018.

Abstract

There is an increasing need to evaluate concentrations of nanoparticles in occupational settings due to their potential negative health effects. The Nanoparticle Respiratory Deposition (NRD) personal sampler was developed to collect nanoparticles separately from larger particles in the breathing zone of workers, while simultaneously providing a measure of respirable mass concentration. This study compared concentrations measured with the NRD sampler to those measured with a nano Micro Orifice Uniform-Deposit Impactor (nanoMOUDI) and respirable samplers in three workplaces. The NRD sampler performed well at two out of three locations, where over 90% of metal particles by mass were submicrometer particle size (a heavy vehicle machining and assembly facility and a shooting range). At the heavy vehicle facility, the mean metal mass concentration of particles collected on the diffusion stage of the NRD was 42.5 ± 10.0 μg/m^3, within 5% of the nanoMOUDI concentration of 44.4 ± 7.4 μg/m^3. At the shooting range, the mass concentration for the diffusion stage of the NRD was 5.9 μg/m^3, 28% above the nanoMOUDI concentration of 4.6 μg/m^3. In contrast, less favorable results were obtained at an iron foundry, where 95% of metal particles by mass were larger than 1 μm. The accuracy of nanoparticle collection by NRD diffusion stage may have been compromised by high concentrations of coarse particles at the iron foundry, where the NRD collected almost 5-fold more nanoparticle mass compared to the nanoMOUDI on one sampling day and was more than 40% different on other sampling days. The respirable concentrations measured by NRD samplers agreed well with concentrations measured by respirable samplers at all sampling locations.

Overall, the NRD sampler accurately measured concentrations of nanoparticles in industrial environments when concentrations of large, coarse mode, particles were low.

Keywords: iron foundry; NRD sampler; nanoMOUDI; nanoparticle mass concentration; respiratory deposition curve; shooting range; welding fume

Introduction

Nano-sized (smaller than 100 nm) aerosols constitute a significant part of particulate matter (PM) generated by many industrial processes such as welding, metal melting, and pouring (Antonini, 2003; Peters *et al.*, 2009). Nanoparticles can effectively deposit throughout the human respiratory track and are known to translocate to the circulatory system and various organs when not cleared effectively by the mucocilliary escalator (Antonini, 2003; Schulte *et al.*, 2009). Exposure to incidental nanoparticles has been associated with various adverse health effects in workers, including eye and respiratory irritation, metal fume fever, obstructive lung disease, and possible neurological changes (Schulte *et al.*, 2009; Simkó and Mattsson, 2010). Therefore, exposure to nanoparticles in occupational settings needs to be assessed and monitored to prevent adverse health outcomes (Asbach *et al.*, 2017).

The industrial hygiene community typically assesses PM exposures using samplers that reflect physiological penetration of particles into different regions of the respiratory tract (inhalable, thoracic, and respirable fractions) (Vincent, 2012). Personal samplers have been developed to assess the exposure of workers to PM in occupational settings according to inhalable, thoracic, or respirable conventions (Koehler and Peters, 2015; L'Orange *et al.*, 2016; Anthony *et al.*, 2017). Inhalable samplers, such as the IOM personal sampler (SKC Inc., Eighty Four, PA, USA) and Button Aerosol Sampler (SKC Inc.) collect particles up to 100 µm in size, with sampling efficiencies ranging from 100% for 1 µm particles to 50% for 100 µm particles. Respirable samplers typically rely on a cyclone inlet to remove particles that cannot pass through the bends of the respiratory system upstream of the alveolar region. The 50% collection efficiency diameter of a respirable cyclone is 4 µm (d_{50}) with all particles larger than 10 µm removed from the sample.

Recently, several samplers have been developed to assess personal exposure to nanoparticles, namely particles with diameters less than 100 nm (Koehler and Peters, 2015; Asbach *et al.*, 2017). The Personal Nanoparticle Sampler (PENS) can measure respirable particle and nanoparticle exposures separately by employing a respirable cyclone and a micro-orifice impactor with d_{50} of 4 µm and 100 nm, respectively (Tsai *et al.*, 2012). Another example, the Nanoparticle Respiratory Deposition (NRD) sampler (Zefon International, Inc., Ocala, FL, USA), uses a respirable cyclone (d_{50} = 4 µm) and a three-jet impactor (d_{50} = 300 nm) to remove large particles, followed by porous polyurethane foam (Mines *et al.*, 2016) to collect nanoparticles by diffusion.

The collection efficiency curve for the diffusion stage in the NRD sampler follows the nanoparticulate matter (NPM) criterion (Cena *et al.*, 2011). The NPM criterion represents the fraction of particles smaller than 300 nm that would deposit in the respiratory system of an average adult under light exercise and nose-breathing conditions. Based on the NPM criterion, the collection efficiency of the diffusion stage of the NRD is 50% for 40 nm particles (d_{50} = 40 nm) increasing to almost 100% for the smallest nanoparticles (<5 nm) and decreasing to 6% for the 500 nm particles (Cena *et al.*, 2011). Deposition of particles in the NRD sampler and in the respiratory system increases due to interception for highly non-spherical particles, such as welding fume or chain-like agglomerates (Park *et al.*, 2015; Mines *et al.*, 2016). The NPM criterion, designed to represent deposition of near-spherical nanoparticles, can be adjusted for such particles using an appropriate dynamic shape factor.

The NRD sampler enables the simultaneous measurement of both nanoparticle dose and respirable exposures. The mass concentration of nanoparticles smaller than 300 nm that would deposit in the average human respiratory tract is calculated as the mass of particles collected on the diffusion stage divided by the air volume sampled. Respirable mass concentration is calculated as the sum of mass collected on the impactor, diffusion stage, and final filter divided by the air volume sampled. Thus far, only the diffusion stage of the NRD sampler has been used to collect welding fumes in laboratory settings, and the mass fraction of selected metal nanoparticles in welding fumes has been determined using a second reference sampler operated beside and simultaneously with the NRD sampler (Cena *et al.*, 2014). In that work, the fume generated by a robotic welding arm was found to have ~30% of manganese (Mn), ~50% of chromium (Cr), and ~ 60% of nickel (Ni) attributed to nanoparticles (collected by the diffusion stage of the NRD sampler) (Cena *et al.*, 2014).

Since the mass concentration of nanoparticles is usually very small, the limits of detection (LODs) and quantification (LOQs) can obscure quantification of nanoparticles in workplace environments with low PM concentrations. Porous polyurethane foam was found to be more suitable than eight nylon meshes as a substrate used in the diffusion stage of the NRD sampler with respect to elemental metal content, particle collection by size, and pressure drop (Mines *et al*., 2016). With the exception of cadmium (Cd), porous polyurethane foam had substantially lower background concentrations than nylon meshes for Cr, copper (Cu), iron (Fe), Mn, Ni, titanium (Ti), and zinc (Zn) (Mines *et al*., 2016). Measurements of nanoparticle concentrations collected by NRD samplers in occupational settings with different aerosol types and concentrations are needed to test the performance of the NRD sampler in industrial settings.

The present study aims to evaluate concentrations of nanoparticles in several occupational settings using the NRD sampler. At three industrial facilities, personal and area concentrations measured with the NRD sampler were compared to those measured by reference samplers. Thus, this work provides insight into exposures to metal nanoparticles in three different settings and evaluates whether the NRD sampler is adequate to directly assess nanoparticle concentrations apart from larger particles in the workplaces.

Materials and Methods

Test sites

Aerosol concentrations and particle size distributions were measured at three occupational sites with substantial concentrations of metal and metal oxide PM (Table 1). These three sites provided varied metal sources to test the NRD sampler performance across a wide range of PM concentrations and with varied background of non-nanoparticle aerosols. The first site was a heavy vehicle machining and assembly facility, where metal and metal oxide PM including nanoparticles were generated by robotic and manual gas metal arc welding (GMAW). The second site was an indoor shooting range with metal-containing nanoparticles produced due to firing of M4 rifles loaded with plastic training ammunition. The last site was an iron foundry that manufactured ductile iron and grey iron metal parts, and monitoring was conducted during metal melting, metal pouring, and grinding operations.

Area sampling from a field sampling cart (Supplementary Fig. 1, available at *Annals of Work Exposure and Health* online) was carried out at the heavy vehicle machining and assembly facility over 3 days averaging 5.9 h/ day. Day 1 sampling occurred near robotic welding, Day 2 sampling was near manual welding and grinding, and Day 3 sampling was between manual and robotic welding operations.

Both area and personal sampling were conducted at the shooting range in 1 day. The field sampling cart was placed ~3 m behind a line of shooters (13 shooters total) and all area sampling equipment was operated simultaneously for 253 min. Personal NRD samplers were positioned in the breathing zones of the shooting instructors, and personal sampling pumps attached to the NRD samplers were operated for a total of 227 and 252 min for two instructors. The pumps were paused during breaks and when instructors exited the shooting range.

Area and personal sampling were also conducted at the iron foundry on three days. The field cart was positioned in the grinding area on Day 1 (491 min), then it was moved next to metal melt and pouring area for Day 2 (449 min) and Day 3 (465 min) sampling. Ductile iron was produced on Days 1 and 2, while grey iron was produced on Day 3. In addition, four workers wore paired NRD and respirable samplers during each of three days (12 paired samples). The job titles for these participants included grinders, metal pourers, delivery workers (who pull transport vessels with melted iron to pouring stations), degating workers (who remove runners, gates, and risers left from channels delivering melted iron to the molds), fork lift operators, and molding machine operators.

Table 1. Sampling sites description and a total number of samplers used at each site.

Site	Processes	Days of sampling	NRD samplers	Respirable samplers
Heavy vehicle machining and assembly facility	Robotic and manual metal arc welding, metal grinding	3	6	3
Shooting range	Firing M4 rifle with plastic training ammunition	1	3	1
Iron foundry	Metal melting and pouring, metal grinding	3	15	15

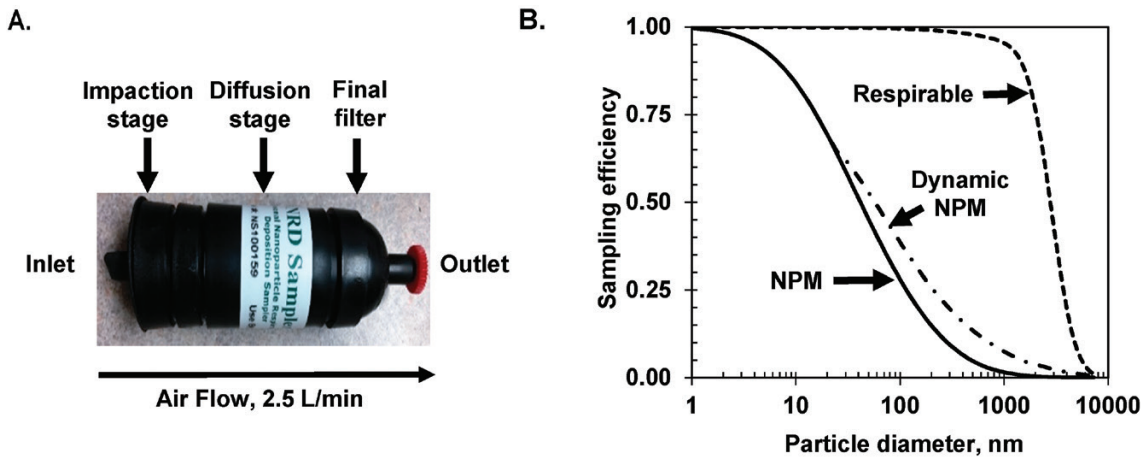

Figure 1. NRD sampler overview (A) and sampling efficiency by particle size (B). The inlet is capped in (A) and the cap is replaced with a respirable cyclone before sampling. NPM criterion represents deposition efficiency of nanoparticles in the respiratory tract. The dynamic NPM criterion indicates adjustment to the NPM criterion using a dynamic shape factor (Kim *et al.*, 2009) for the highly non-spherical particles such as chain agglomerates. The respirable curve as defined by ACGIH represents the particles that can penetrate into the deep lung.

Sampling equipment

NRD sampler

The NRD sampler has three main components: an impactor, a diffusion stage, and a final filter (Fig. 1A). Its operation requires a 2.5 L min^{-1} sampling rate to draw air into the upstream aluminum cyclone used to remove non-respirable particles. Air and particles passing through the cyclone reach the impaction stage. The impactor removes respirable particles larger than 300 nm from the air stream, which in this study were collected and analyzed as a contribution to respirable mass concentration. To allow for this analysis, polycarbonate membrane filters (PCTE, 0.2 µm pore size, 47 mm diameter, Sterlitech Corporation, Kent, WA, USA) were cut in-house to 9 mm circles and attached to the center of the impactor plate. A round stamp cut out of foam (37 mm in diameter) and dipped into Heavy-Duty Silicon Oil (part # 07041, MSP Corporation, Shoreview, MN, USA) was pressed onto the middle of polycarbonate substrates to create a layer of silicone oil coating. Greased substrates were baked in the oven at 50°C for 4 h to evaporate volatile material and create a thin layer of sticky silicone intended to prevent particle bounce (Pak *et al.* 1992). Particles remaining airborne then passed through a 25-mm-diameter and 40-mm-long polyurethane foam cylinder, which collects particles smaller than 300 nm with an efficiency matching the NPM sampling criterion (Fig. 1B). A mixed cellulose ester (MCE) filter (0.8 µm pore size, 25 mm diameter, Zefon International, Inc.) was used as the final NRD stage to collect all remaining particles in the sampled air.

Reference sampling equipment

Reference mass concentrations were measured with respirable samplers and a cascade impactor (nanoMOUDI, Model 125-R, MSP Corporation). The respirable samplers consisted of an aluminum respirable cyclone (25 mm, SKC Inc.) with a two-piece cassette holding an MCE filter (0.8 µm pore size, 25 mm diameter, Zefon International, Inc.). Respirable samplers were placed next to NRD samplers on the field cart (Supplementary Fig. 1, available at *Annals of Work Exposure and Health* online) or on workers. Personal sampling pumps (GilAir Plus, Sensidyne, St. Petersburg, FL, USA) used for NRD and respirable samplers were calibrated with an air flow calibrator (TetraCal, Mesa Labs, Butler, NJ, USA) before and after sample collection.

The nanoMOUDI was placed on the field cart so that its inlet was at the same level with the cyclones for NRD and respirable samplers (Supplementary Fig. 1, available at *Annals of Work Exposure and Health* online). The nanoMOUDI was operated at 10 L min^{-1}, and 13 polycarbonate substrates (PCTE, 0.2 µm pore size, 47 mm diameter, Sterlitech Corporation) coated with silicon oil, using the same procedure described above for NRD impactors, were used for particle collection. An MCE filter (0.8 µm pore size, 47 mm diameter, Zefon International, Inc.) was used as a backup filter in the last nanoMOUDI stage.

A scanning mobility particle sizer (SMPS) (NanoScan, Model 3910, TSI Inc., Shoreview, MN, USA) on the field cart measured particle number concentration by size from 10 to 410 nm (mobility diameters) every minute of

sampling. An electrostatic precipitator (ESPnano, model 100, DASH Connector Technology, Inc., WA, USA) was used to collect particle deposits on transmission electron microscope (TEM) grids (200-mesh carbon coated Ni grid, 01840N-F, Ted Pella Inc., CA, USA) 2–3 times per day in order to evaluate primary particle diameter, nanoparticle morphology, and agglomeration state. TEM images were acquired using TEM (JEOL-1230, JEOL Ltd., Japan) and analyzed by ImageJ software (version 1.50i, NIH, USA).

Chemical analysis by Inductively Coupled Plasma-Mass Spectrometry (ICP-MS)

NRD samples (impactor substrates, diffusion stages, and final filters), respirable filters, and nanoMOUDI substrates were digested separately using a Microwave Reaction System (MARS 6, CEM Corporation, Matthews, NC, USA) following the NIOSH method 7302 (Ashley, 2016). After digestion, the samples were diluted with milliQ water to 2% HNO_3 solutions. ICP-MS (iCAP RQ ICP-MS, Thermo Fisher Scientific, Waltham, MA, USA) analysis was carried out for Cu, Fe, Mn, lead (Pb), Zn, antimony (Sb), barium (Ba), and aluminum (Al) present in Complete Standard Solution 71A and Refractory Elements Standard Solution 71B using an Internal Standard Solution 71D. All solutions were National Institute of Standards and Technology (NIST) certified reference materials sold by Inorganic Ventures (Christiansburg, VA, USA). Standard solutions were diluted with 2% HNO_3 (Trace Metal Grade, Fisher Scientific LLC, Pittsburgh, PA, USA) to concentrations of 0.5, 1, 2, 5, 10, 20, 50, 100, 200, and 500 µg/l to measure the calibration curve. LOD for each metal in all substrates was determined as 3σ above the mean blank signal, where σ represents the standard deviation (SD) of the blank signal. LOQ was calculated as a mean blank signal plus 10σ.

Adjustments to nanoMOUDI concentrations

NPM and respirable collection efficiency criteria, shown in Fig. 1B, were applied to the mass concentrations $C(i)$ measured by ICP-MS for each nanoMOUDI stage i, and then added together to obtain NPM (C_{NPM}) and respirable (C_{resp}) concentrations for the nanoMOUDI measurements, as shown in Equations 1 and 2:

$$C_{NPM} = \sum_{i=1}^{14} NPM(i) \times C(i) \quad (1)$$

$$C_{resp} = \sum_{i=1}^{14} Resp(i) \times C(i) \quad (2)$$

where NPM(i) and Resp(i) are the NPM and respirable sampling efficiencies averaged over the size range corresponding to each nanoMOUDI stage i.

Statistical analysis

A paired t-test was conducted to compare means of NRD diffusion stage and NPM adjusted nanoMOUDI concentrations measured at the heavy vehicle machining and assembly center and the iron foundry. For personal NRD samplers from the iron foundry with diffusion stage concentrations below the LOD, the LOD/2 for Fe was assigned to calculate the mean and SD, as it was detected most consistently across the foundry samples, contributing to >85% of the sample mass. Similar tests compared the means of respirable concentrations measured by the NRD with nanoMOUDI and respirable samplers. All tests compared significance at $\alpha = 0.05$.

Results and Discussion

Heavy vehicle machining and assembly facility

The main metal-generating processes at the heavy vehicle machining and assembly facility were metal-arc welding and grinding. TEM images revealed chain-like agglomerates of nanoparticles present on all TEM samples collected at this sampling site (Fig. 2). These morphologies are expected and consistent with observations by other groups for laboratory-generated and industrial welding fume (Stephenson *et al.*, 2003; Park *et al.*, 2014). The primary particle diameters ranged from smaller than 10 nm to over 100 nm as can be seen in Fig. 2A. We hypothesize that the elemental composition varies for small and large primary particles, and this will be discussed in details in a follow-up manuscript. The important observation from TEM images is that the primary nanoparticles form chain-like agglomerates, necessitating adjustment of the NPM criterion using a dynamic shape factor (Fig. 1B) (Kim *et al.*, 2009).

NanoMOUDI stages, NRD parts, respirable filters, and blanks from heavy vehicle machining and assembly facility were analyzed for metals by ICP-MS. Concentrations of Mn, Fe, and Cu were above the LOQs (LOQs and LODs for all substrates are shown in the Supplementary Table 1, available at *Annals of Work Exposure and Health* online) in the samples collected at the vehicle machining and assembly facility. The mass concentrations of these three metals were added together to obtain 'metal' mass concentrations. As shown in Fig. 3, most of the particles collected by nanoMOUDI stages were in the size range from 50 to 1000 nm, with a peak diameter around 200 nm, which is in agreement with the sizes of agglomerates observed from TEM images shown in Fig. 2. The number concentrations by size measured with the NanoScan SMPS were bimodal with primary mode peak diameter at 141 ± 22 nm for all

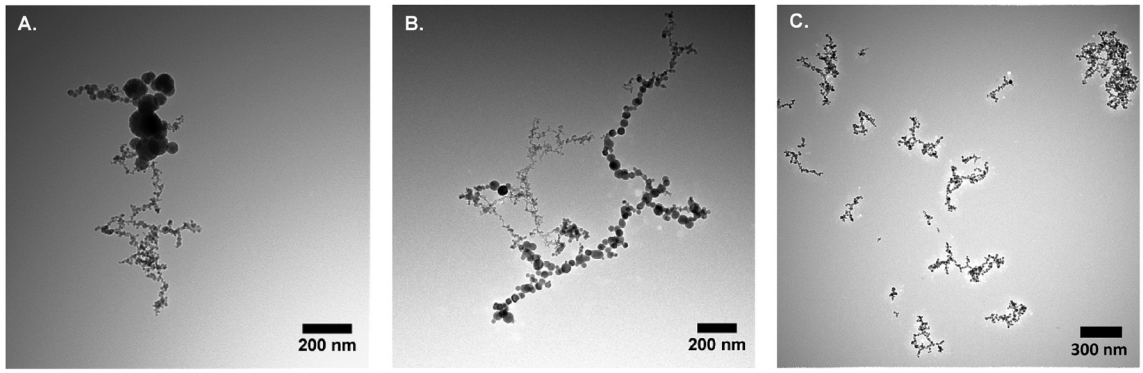

Figure 2. Representative TEM images of particles collected in the heavy vehicle machining and assembly facility on Days 1–3 (A–C). Different shapes and sizes of nanoparticle agglomerates were observed.

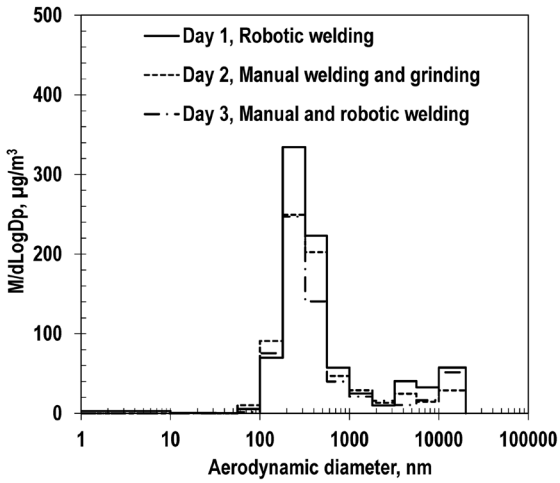

Figure 3. Metal mass concentrations measured on the nanoMOUDI substrates collected at the heavy vehicle machining and assembly facility on three sampling days.

three sampling days (Supplementary Fig. 2, available at *Annals of Work Exposure and Health* online).

Table 2 compares the metal mass concentrations measured by the NRD to reference samplers. Each NRD concentration in Table 2 represents an average of concentrations measured from two NRD samplers located next to each other on the field-sampling cart. There were no personal measurements taken at this sampling site. There was no significant difference in the mean mass concentration measured with the NRD diffusion stage (mean ± SD; 42.5 ± 10.0 µg/m^3) and the nanoMOUDI concentration calculated using Equation 1 (44.4 ± 7.4 µg/m^3) (P = 0.46), suggesting that the NRD diffusion stage properly separates nanoparticles from the respirable PM. The mean of respirable concentrations measured with the NRD sampler (214 ± 47 µg/m^3) was not significantly different from those measured with respirable samplers (269 ± 29 µg/m^3) (P = 0.06), indicating that the NRD provides a reasonable estimate of respirable mass concentration when all stages are added together. Although not significantly different, respirable concentrations measured by NRDs were consistently lower than those measured with the respirable samplers (Table 2), indicating that some PM losses may occur on the interior walls of NRD samplers. In contrast, the mean respirable concentrations measured with the NRD were consistently higher than those from the nanoMOUDI concentrations calculated using Equation 2 (P = 0.048) (Table 2). One plausible, and most likely, explanation for this difference is PM losses on the back sides of nanoMOUDI nozzle plates, as was visually observed after sampling (Supplementary Fig. 3, available at *Annals of Work Exposure and Health* online).

Shooting range

Figures 4A and B show representative TEM images of samples collected at the shooting range. Single nanoparticles with diameters around 10 nm and small agglomerates up to 70 nm in size were observed. The distribution of primary particles' diameters is shown in Fig. 4C, with the diameter of most primary particles ranging from few nanometers to 25 nm.

Pb, Fe, Zn, Sb, Ba, Al, and Cu were detected by ICP-MS in the samples collected at the shooting range. The metal mass concentration by size is shown in Fig. 5. Most of the nanoMOUDI stages collected very low metal concentrations ranging from 0.2 to 13.5 µg/m^3, with substantial concentrations (>2 µg/m^3) measured on stages collecting large (100–900 nm diameter) particles (Fig. 5). We suspect that these larger particles are the agglomerates of the primary particles observed in TEM images. A metal mass concentration of 2.2 µg/m^3

Table 2. Comparison of metal mass concentrations measured by ICP-MS with the NRD, the nanoMOUDI, and respirable sampler at the heavy vehicle machining and assembly facility. Each NRD concentration represents an average measured from two samplers located next to each other.

	NRD Sampler				NanoMOUDI		Respirable concentration µg/m³
	Diffusion stage µg/m³	Impaction stage µg/m³	Final filter µg/m³	Respirable concentration µg/m³	NPM adjusted µg/m³	Respirable concentration µg/m³	
Day 1	**50.7**	**49.4**	**160.3**	**260.5**	51.9	186.5	301.6
Day 2	45.3	44.0	126.8	216.1	44.0	160.8	256.0
Day 3	31.4	30.9	103.8	166.1	37.2	134.5	248.9
Mean ± SD	42.5 ± 10.0	40.2 ± 13.1	132 ± 40	214 ± 47	44.4 ± 7.4	161 ± 26	269 ± 29

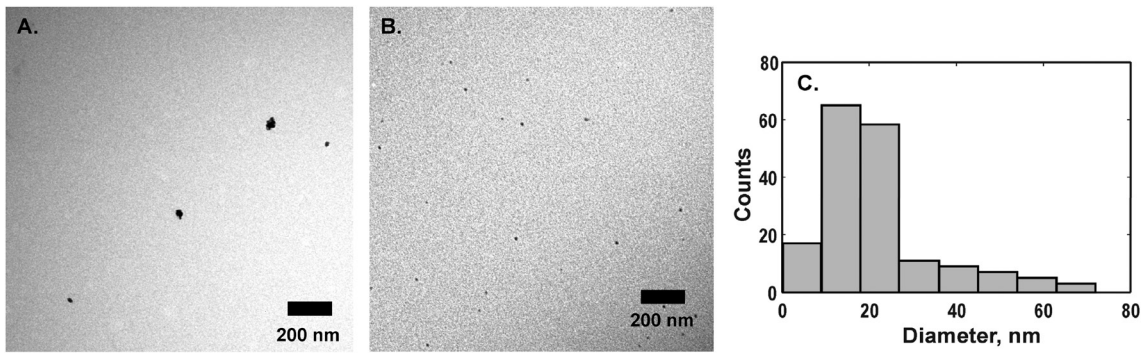

Figure 4. TEM images of samples collected at the shooting range (A, B). These images are representative of over a dozen images acquired for this location. Small agglomerates (A) or single nanoparticles (B) were observed at the shooting range. A histogram of 180 particle diameters measured from different TEM images in ImageJ software (C).

was also measured for particles in the size range from 10–20 nm. These are most likely single nanoparticles observed in TEM images shown in Fig. 4. Their mass concentration is much smaller compared to particles larger than 100 nm, but their particle counts (up to 2×10^6 particle/cm^3) were substantial as measured by NanoScan SMPS (Supplementary Fig. 4, available at *Annals of Work Exposure and Health* online).

The NanoScan SMPS revealed different particle number concentrations during morning and afternoon sampling at the shooting range (Supplementary Fig. 4, available at *Annals of Work Exposure and Health* online). There were fewer shots fired in the morning because instruction increased the intervals between the shots, compared to the afternoon. The particle number concentration by size measured by NanoScan SMPS in the morning hours had a single mode distribution with a peak diameter around 40 nm (Supplementary Fig. 4, available at *Annals of Work Exposure and Health* online). The particle number concentrations increased significantly after the lunch break, following the increase in the frequency of shooting. The particle number concentration

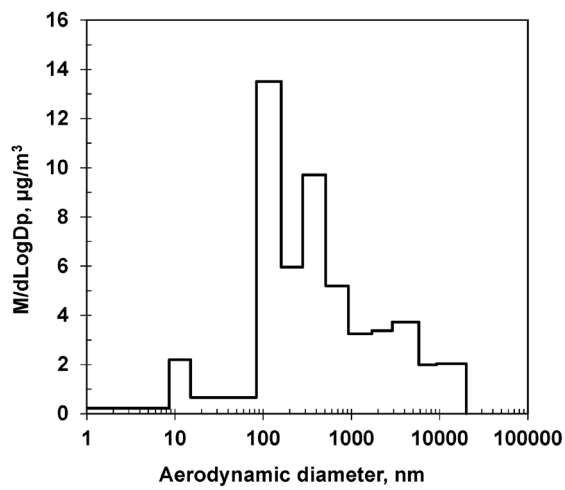

Figure 5. Metal mass concentration by size measured on the nanoMOUDI substrates from the shooting range.

by size in the afternoon was bimodal with a second peak at 150 nm (Supplementary Fig. 4, available at *Annals of Work Exposure and Health* online). This observation

confirms the aggregation of nanoparticles due to high PM concentrations produced by the intensive firing in the afternoon, therefore the NPM criterion adjusted by dynamic shape factor calculated following Kim *et al.* (2009) (Fig. 1B) was applied to estimate NPM fraction of nanoparticles collected in the nanoMOUDI stages.

Table 3 summarizes metal mass concentrations measured by NRD, nanoMOUDI, and respirable samplers deployed at the shooting range. Three NRD samplers (one area and two personal samplers) were simultaneously deployed with one respirable sampler (area) and one nanoMOUDI (area). In area sampling, the nanoparticle mass concentration measured with the diffusion stage of the NRD (5.9 μg/m^3) was 28% higher than that measured with the nanoMOUDI (4.6 μg/m^3). The respirable concentration measured with the NRD sampler was 17.1 μg/m^3, within 6% of the respirable sampler concentration (18.1 μg/m^3). In contrast, the respirable mass concentration estimated from nanoMOUDI data (13.3 μg/m^3) was substantially lower than concentrations measured with the NRD and respirable samplers. Again, we speculate that particle losses in the nanoMOUDI account for this difference. The personal samples yielded similar concentrations to area samples (Table 3).

Iron foundry

The iron foundry was visibly the 'dirtiest' of three sampling sites covered in this study. Many metal-generating processes were operating simultaneously, with a substantial proportion of the PM larger than the 10 μm upper limit of the respirable sampling. Particle size and morphology identified through TEM varied across sampling locations (Fig. 6). The grinding area had single particles and agglomerates up to 400 nm (Fig. 6A), but location near the transport vessels with melted iron had chain-like agglomerates of nano-sized particles similar to welding fume (Fig. 6B). Near a molder, where sand forms were prepared, different profiles were observed (Fig. 6C), although no evidence of particles larger than 1000 nm were observed in the ESPnano samples.

The most concentrated metals detected at the foundry by ICP-MS were Fe, Mn, Zn, and Cu. The metal mass concentrations by size and sampling day measured with the nanoMOUDI are shown in Fig. 7. Compared to the other sites visited in this study, mass concentrations were substantially greater and shifted to larger particle sizes in the foundry. Little mass was detected in the nanometer size range. The mass concentrations of submicrometer particles were substantially lower in the

Table 3. Comparison of metal mass concentrations measured by ICP-MS with the NRD, the nanoMOUDI, and respirable sampler at the shooting range.

	NRD Sampler				NanoMOUDI		Respirable concentration μg/m^3
	Diffusion stage, μg/m^3	Impaction stage, μg/m^3	Final filter, μg/m^3	Respirable conc., μg/m^3	NPM adjusted, μg/m^3	Respirable conc., μg/m^3	
Area	5.9	6.5	4.7	17.1	4.6	13.3	18.1
Personal 1	4.3	6.8	3.2	14.3			
Personal 2	8.3	7.8	3.2	19.3			

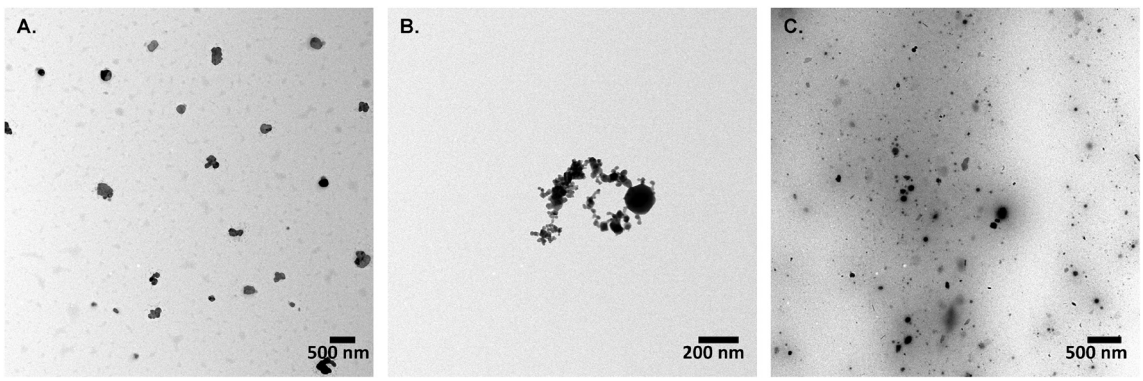

Figure 6. Representative TEM images of samples collected at the iron foundry in grinding area (A), near iron melting (B), and near molding (C). Different shapes and sizes of agglomerates were observed.

grinding area (Day 1) than in the melt and pouring area (Days 2 and 3). Moreover, within the metal melt and pouring area, the mass concentration of submicrometer particles was substantially lower on Day 2 than on Day 3, which could relate to different ventilation settings and/or different material being produced (ductile iron on Day 2 and grey iron on Day 3). The study of the composition of particles collected at the iron foundry will be published in a separate manuscript. Particle number concentrations by size measured by NanoScan SMPS at the iron foundry showed that particles were present in the size range from 10 to 300 nm with the total number concentrations between 10^4 and 10^5 particles/cm^3 (Supplementary Fig. 5, available at *Annals of Work Exposure and Health* online), although their mass is negligible compared to the larger particles. Due to an abundance of large agglomerates, NPM criterion calculated using dynamic shape factor following Kim *et al.* (2009) as shown in Fig. 1B was applied to estimate the NPM fraction of nanoparticles collected on the nanoMOUDI stages (Table 4).

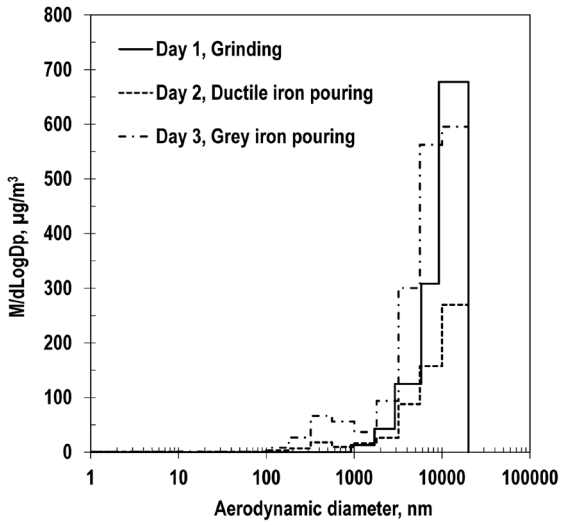

Figure 7. Metal mass concentrations measured on the nanoMOUDI substrates collected at the iron foundry on three sampling days.

Table 4 summarizes metal mass concentrations for the area samplers (NRD samplers, nanoMOUDI, and respirable samplers) deployed at the iron foundry. The impaction stage of the NRD sampler had the highest concentration of metals, confirming that fine and coarse particles constituted the largest fraction of PM. Respirable concentrations were similar for Days 1 and 2 and almost 3-fold higher on Day 3. Particle number concentrations measured with the NanoScan SMPS showed a similar trend by sampling day (Supplementary Fig. 5, available at *Annals of Work Exposure and Health* online). There was no statistical difference between the mean respirable concentrations measured by the NRD (77.5 ± 46.3 µg/m^3) and respirable samplers (74.1 ± 52.8 µg/m^3) (P = 0.49). As observed at previous sites, the nanoMOUDI respirable concentrations (61.0 ± 46.7 µg/m^3) were substantially lower than those obtained from the NRD and respirable samplers (P = 0.0008), again presumably due to inter-stage losses.

In contrast to the other sites, nanoparticle mass concentrations measured with the NRD diffusion stage compared poorly to those measured with the nanoMOUDI. On Day 1 in the grinding area, the NPM adjusted nanoMOUDI concentration was only 2.1 µg/m^3 compared to the NRD diffusion stage value of 10.2 µg/m^3. We speculate that the large particles at this site may have caused the impaction substrate in the NRD to overload, allowing some particles larger than the cutoff size of the impactor to pass onto the diffusion stage. This suggests that a high concentration of coarse and fine particles could be a limitation for measuring nanoparticle concentrations with the NRD sampler.

Table 4. Comparison of metal mass concentrations measured by ICP-MS with the NRD, the nanoMOUDI, and respirable sampler at the iron foundry.

	NRD Sampler				NanoMOUDI		Respirable concentration µg/m^3
	Diffusion stage µg/m^3	Impaction stage µg/m^3	Final filter µg/m^3	Respirable concentration µg/m^3	NPM adjusted µg/m^3	Respirable concentration µg/m^3	
Day 1	**10.2**	**36.4**	**3.7**	**50.4**	**2.1**	34.4	46.0
Day 2	7.5	37.5	6.1	51.1	4.6	33.7	41.2
Day 3	8.0	101	22.0	131	14.1	115	135
Mean ± SD	8.6 ± 1.4	58.3 ± 37.0	10.6 ± 9.9	77.5 ± 46.3	6.9 ± 6.3	61.0 ± 46.7	74.1 ± 52.8

In the melt and pouring area, the NRD diffusion stage concentrations were 7.5 and 8.0 µg/m^3 (Days 2 and 3, respectively), whereas the matched NPM adjusted nanoMOUDI concentrations were 4.6 and 13.7 µg/m^3. Since we observed much higher particle number concentrations measured by the NanoScan SMPS on Day 3 than on Day 2 (Supplementary Fig. 5, available at *Annals of Occupational Hygiene* online), we expected nanoparticle mass have the same tendency since sampling times were nearly the same on these days. Nanoparticle mass concentrations from the nanoMOUDI were consistent with our expectation (3-fold higher on Day 3), whereas those from the NRD diffusion stages for the 2 days were similar. This may be indicative of high concentrations of large particles preventing accurate measurement of nanoparticles using the NRD sampler, suggesting further investigation is warranted.

A pair of personal NRD and respirable samplers was worn by 12 workers in different locations within the iron foundry (Table 5). The mass concentration derived from the NRD diffusion stage varied between 2.4 (Fe LOD/2) and 37.2 µg/m^3 with a mean of 14.4 ± 10.1 µg/m^3. There was no clear trend in the diffusion stage concentrations by location. The NRD impaction stage concentration was the highest among NRD parts at all locations, indicating that particles larger than 300 nm constitute the largest fraction of PM. Respirable cyclones fell off the inlets of two NRD samplers worn by Grinder 1 and Delivery worker 3 due to quick and sharp movements leading to collection of particles larger than respirable size. Respirable concentrations varied between 17.2 and 121 µg/m^3 (excluding two workers mentioned above) for the NRD samplers and between 12.9 and 158 µg/m^3 for the respirable samplers. Mean respirable concentration measured with personal NRDs was 69.4 ± 34.5 µg/m^3 (excluding Grinder 1 and Delivery worker 3), and was not statistically different from 76.8 ± 53.5 µg/m^3, measured with paired personal respirable samplers (P = 0.59).

The nanoparticle-to-respirable fraction was calculated as the NRD diffusion stage concentration divided by the sum of all NRD stages (respirable concentration; Table 5). The personal sampling results from the iron foundry indicated that workers located at the pouring stations were exposed to a higher mean nanoparticle fraction of PM of 0.22 ± 0.02, whereas the mean nanoparticle fraction for all other workers was 0.14 ± 0.04 (excludes three <LOD concentrations) (Table 5). The finding that the fraction of nanoparticles was higher for the pourers was expected because these workers are frequently in close proximity of hot molten metal. Therefore, the NRD

Table 5. Comparison of metal mass concentrations measured by ICP-MS with personal NRD and respirable samplers at the iron foundry.

Worker job title	NRD Sampler				Nanoparticle-to-respirable fraction	Respirable sampler µg/m^3
	Diffusion stage µg/m^3	Impaction stage µg/m^3	Final filter µg/m^3	Respirable concentration µg/m^3		
Degating worker	21.1	92.9	6.8	121	0.17	108
Grinder 1	37.2	200.2[b]	18.1	256[b]	0.15	136[d]
Grinder 2	7.7	56.8	3.3	67.9	0.11	72.2
Fork lift operator	<LOD	24.3	0.1	24.4	<LOD	35.9
Molding machine 1	<LOD	14.1	3.1	17.2	<LOD	12.9
Molding machine 2	14.2	45.6	28.5	88.3	0.16	66.6
Pourer 1	18.9	46.5	30.9	96.3	**0.20**	174
Pourer 2	16.9	50.5	6.1	73.5	**0.23**	35.3
Pourer 3	22.0	60.7	10.6	93.3	**0.24**	54.1
Delivery worker 1	<LOD	25.9	4.7	30.7	<LOD	51.2
Delivery worker 2	11.1	33.1	36.7	81.0	0.14	158
Delivery worker 3	15.6	86.4[b]	33.5	136[b]	0.11	109[d]
Mean ± SD	14.4 ± 10.1[a]	45.0 ± 22.6[c]	15.2 ± 13.6	69.4 ± 34.5[c]		76.8 ± 53.5[d]

[a]For samples < LOD, the LOD/ $\sqrt{2}$ for Fe was assigned to calculate the mean and SD, as it was detected most consistently across all foundry samples, contributing to >85% of the sample mass.

[b]Samplers' cyclones fell off during sampling leading to larger particles collection on the impaction stage and overestimation of respirable concentration.

[c]Personal values marked with [b] were not included in the mean due to cyclones detachment during sampling.

[d]Personal values marked with [d] were not included in the mean for side-by-side comparison with NRD respirable concentrations.

sampler could be a valuable tool in assessing the fraction of nanoparticles compared to larger respirable particles. Such information could be used to take actions for reducing exposures to nanoparticles based on individual worker's location and/or job title.

Conclusions

In summary, respirable mass concentrations measured with the NRD sampler were within 6% of the respirable sampler concentrations at shooting range and iron foundry and within 20% at heavy vehicle machining and assembly facility. Moreover, nanoparticle concentrations measured with the NRD sampler were similar to those measured with the nanoMOUDI reference sampler at sites dominated by submicrometer particles. For example, the mean nanoparticle concentration measured with the NRD sampler was within ±5% of that measured with the nanoMOUDI at the heavy vehicle machining and assembly facility. However, agreement in nanoparticle concentrations measured with the NRD sampler and nanoMOUDI was considerably poorer in the iron foundry where mass concentrations were dominated by coarse particles (larger than 1 μm) with ultrafine and fine particles only contributing less than 5% of total metal mass. The reason for the poorer agreement has not been definitively determined but one possible reason is overload of the NRD impactor and transport of larger particles to the diffusion substrate, thereby giving an overestimation of nanoparticle concentration. The samples collected at the other two sampling sites did not show this behavior. Further work is needed to investigate and resolve particle bounce in the impactor. The effectiveness of the NRD sampler for nanotubes and fibers has not been evaluated in this work and will be a subject of a future work. A better connection is needed to prevent detachment of the respirable cyclone from the impactor of the NRD during field measurements. In conclusion, the NRD sampler can be used to accurately measure concentrations of nanoparticles in industrial environments where concentrations of coarse particles are relatively low.

Supplementary Data

Supplementary data are available at *Annals of Work Exposures and Health* online.

Funding

This work utilized the JEOL JEM-1230 Transmission Electron Microscope in the University of Iowa Central Microscopy Research Facilities that was purchased with funding from the NIH SIG grant number 1 S10 RR018998-01. Financial support for this work was provided by National Institute for Occupational Safety and Health grants R01 OH010238 and R01 OH010295.

Acknowledgements

We thank Dr. Craig Holder for arranging sampling at the shooting range and his help with the sampling equipment. The ICP-MS analysis was done in the Environmental Complex Analysis Laboratory on the UC San Diego campus. Its contents, including any opinions and/or conclusions expressed, are solely those of the authors.

Conflict of Interest Statement

The authors declare no conflict of interest relating to the material presented in this article.

References

Anthony TR, Cai C, Mehaffy J *et al*. (2017) Performance of prototype high-flow inhalable dust sampler in a livestock production facility. *J Occup Environ Hyg*; **14**: 313–22.

Antonini JM. (2003) Health effects of welding. *Crit Rev Toxicol*; **33**: 61–103.

Asbach C, Alexander C, Clavaguera S *et al*. (2017) Review of measurement techniques and methods for assessing personal exposure to airborne nanomaterials in workplaces. *Sci Total Environ*; **603-604**: 793–806.

Ashley K. (2016) *Elements by ICP (Microwave Digestion), Method 7302*. U.S. National Institute for Occupational Safety and Health (NIOSH), NIOSH Manual of Analytical Methods, 5th ed. web book. Method 7302, NIOSH, Cincinnati, OH, 2016. www.cdc.gov/niosh/nmam. Accessed 9 May 2018.

Cena LG, Anthony TR, Peters TM. (2011) A personal Nanoparticle Respiratory Deposition (NRD) sampler. *Environ Sci Technol*; **45**: 6483–90.

Cena LG, Keane MJ, Chisholm WP *et al*. (2014) A novel method for assessing respiratory deposition of welding fume nanoparticles. *J Occup Environ Hyg*; **11**: 771–80.

ICRP. (1994) Human respiratory tract model for radiological protection. *International Commission on Radiological Protection (ICRP)*; **66**: 1–3.

Kim SC, Wang J, Emery MS *et al*. (2009) Structural property effect of nanoparticle agglomerates on particle penetration through fibrous filter. *Aerosol Sci Technol*; **43**: 344–55.

Koehler KA, Peters TM. (2015) New methods for personal exposure monitoring for airborne particles. *Curr Environ Health Rep*; **2**: 399–411.

L'Orange C, Anderson K, Sleeth D *et al*. (2016) A simple and disposable sampler for inhalable aerosol. *Ann Occup Hyg*; **60**: 150–60.

Mines LWD, Park JH, Mudunkotuwa IA *et al*. (2016) Porous polyurethane foam for use as a particle collection substrate in a nanoparticle respiratory deposition sampler. *Aerosol Sci Technol*; **50**: 497–506.

Pak SS, Liu BYH, Rubow KL. (1992) Effect of coating thickness on particle bounce in inertial impactors. *Aerosol Sci Technol*; **16**: 141–50.

Park JH, Mudunkotuwa IA, Kim JS *et al*. (2014) Physicochemical characterization of simulated welding fume from a spark discharge system. *Aerosol Sci Technol*; **47**: 768–76.

Park JH, Mudunkotuwa IA, Mines LW *et al*. (2015) A granular bed for use in a nanoparticle respiratory deposition sampler. *Aerosol Sci Technol*; **49**: 179–87.

Peters TM, Elzey S, Johnson R *et al*. (2009) Airborne monitoring to distinguish engineered nanomaterials from incidental particles for environmental health and safety. *J Occup Environ Hyg*; **6**: 73–81.

Schulte PA, Schubauer-Berigan MK, Mayweather C *et al*. (2009) Issues in the development of epidemiologic studies of workers exposed to engineered nanoparticles. *J Occup Environ Med*; **51**: 323–35.

Simkó M, Mattsson MO. (2010) Risks from accidental exposures to engineered nanoparticles and neurological health effects: a critical review. *Part Fibre Toxicol*; **7**: 42.

Stephenson D, Seshadri G, Veranth JM. (2003) Workplace exposure to submicron particle mass and number concentrations from manual arc welding of carbon steel. *AIHA J (Fairfax, Va)*; **64**: 516–21.

Tsai CJ, Liu CN, Hung SM *et al*. (2012) Novel active personal nanoparticle sampler for the exposure assessment of nanoparticles in workplaces. *Environ Sci Technol*; **46**: 4546–52.

Vincent JH. (2012) Occupational and environmental aerosol exposure assessment: a scientific journey from the past, through the present and into the future. *J Environ Monit*; **14**: 340–7.